COMMENTARY

Reemerging role of cable properties in action potential initiation

Yunyong Ma and John R. Huguenard[1]

Department of Neurology and Neurological Sciences, Stanford University School of Medicine, Stanford, CA 94305

It is generally accepted that the axon initial segment (AIS), the neuroanatomical region linking cell body and axon, is the site of action potential (AP) generation in central neurons (1, 2). Because the occurrence, timing, and pattern of APs play critical roles in sensory encoding, motor output, and synaptic plasticity, the mechanisms underlying AP initiation are of fundamental interest. APs are initiated through membrane depolarization driven by the influx of sodium ions (Na^+) through voltage-gated ion channels. The ability of Na currents to produce local depolarization depends on the ratio of the sources and sinks of current flow. Cable theory accounts for current flow down two distinct paths: (*i*) longitudinally along the central conductor and (*ii*) transversely through the cable sheathing or membrane. This theory, initially developed to understand signal losses in transatlantic telegraph cables, is also highly applicable to neuronal membrane compartments, such as axons, dendrites, and cell bodies (3, 4). For AP initiation, the source is Na current, and the sink is the loading resulting from current flow to adjacent membrane compartments, with both resistive and capacitive passive components. According to cable theory, either greater Na^+ influx or lower passive load would increase membrane depolarization and favor local initiation. To date, the role of electrical load has been inferred from the results of computational studies, with little direct support (5–7). In contrast, recent studies on AP initiation have focused on differences in the localized influx of Na currents. According to this view, a region of concentrated local Na^+ influx endows the AIS initiation site with the lowest AP threshold. To evaluate the relative contributions of current source and electrical load in AP initiation, it is pivotal to determine whether the AP initiation site is the location of highest Na current density. If this is not the case, then what factors account for the mismatch? These questions have remained unanswered, largely because of technical constraints of existing AIS recording technologies. In PNAS, Baranauskas et al. (8) combine multiple experimental and theoretical approaches to address this important question and identify a key role of cable properties in determining the site of AP initiation.

In the first set of experiments, by applying simultaneous somatic whole-cell recordings and serial axonal loose-patch recordings, the authors precisely identified the initiation zone of APs. Previous voltage-sensitive dye (VSD) imaging studies had suggested that the trigger zone was preferentially located in the distal region of the AIS (9, 10). Because microelectrode measurements provide precise spatiotemporal resolution, in the present report the authors carried out loose-patch axonal recordings and found the exact position of the initiation region, the most distal 10 μm of the AIS (Fig. 1). This result is qualitatively consistent to previous studies (9, 10) but reveals a narrower and more distal initiation zone.

After determining the precise initiation zone, the authors then aimed to determine whether this region had the highest localized Na current density within the AIS. This is a complicated experimental issue for which direct evidence has been elusive. In what is arguably the most direct approach, voltage clamp of outside-out (11, 12) and conventional cell-attached (13) membrane patches has been used to assess Na current density along the AIS. However, the fidelity of these approaches may be limited by localized geometric factors, such as Na channel anchoring by cytoskeletal elements (14) that may limit channel density in recorded membrane patches. In support of this view is the finding that disruption of the actin cytoskeleton with cytochalasin B increased recorded AIS Na currents (13). A complementary but indirect approach, immunocytochemical staining, has been used to demonstrate regions of high Na channel immunoreactivity along the AIS (15–17), but it is not known whether the intensity of immunoreactivity is linearly related to density of functional Na channels. Besides Na channel density, other channel properties, such as gating, would influence the amplitude of Na current. Conflicting results have been reported. For example, a hyperpolarizing shift in voltage-dependence of Na channel activation in the distal AIS has been reported that would contribute to the AP initiation in distal AIS (11, 12, 17), but this difference in gating has not always been consistently observed (13).

Although the diverse approaches described above have provided some information about

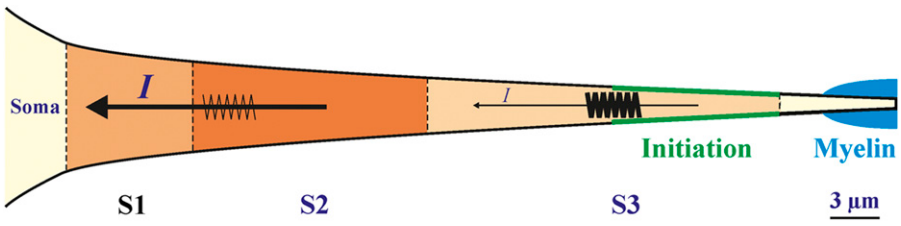

Fig. 1. A schematic cartoon depicting structural components associated the AIS. Darkness indicates intensity of Na^+ fluorescence reflecting axoplasmic Na^+ concentration ([Na^+]). The AIS is functionally divided into three segments with distinct Na^+ profiles (S1–S3) that have average lengths of 8, 14, and 21 μm, respectively. The proximal S1 segment connects to the soma with its large capacitance, but S3 is attached to the downstream myelinated axon that has very minor capacitive load. Compared with the S1 and S2 segments, the S3 region has the lowest density of Na^+ influx but highest axoplasmic resistivity (thick resistor symbol) to the soma, and hence the lowest current load (small I). In contrast, the S2 segment with the highest Na influx has lower axoplasmic resistivity to the soma (thinner resistor symbol), and greater current sink (large I), that presumably prevent local depolarization and AP initiation. As illustrated, the spike initiation site in the AIS is located at the most distal 10-μm region, despite its lower Na current density, because it has highest internal resistance to the large somatic capacitive sink.

Author contributions: Y.M. and J.R.H. wrote the paper.

The authors declare no conflict of interest.

See companion article on page 4051.

[1]To whom correspondence should be addressed. E-mail: john.huguenard@stanford.edu.

Na current distribution and function in the AIS, direct measurement of Na current density has been constrained by the limited spatial resolution and fidelity of existing methodologies. The study by Baranauskas et al. (8) uses a sophisticated technique, high speed Na (HSN) imaging, to directly investigate the distribution of Na current within the AIS. The basic principle of this method is to load individual neurons with a Na^+-sensitive dye, sodium-binding benzofuran isophthalate (SBFI), and then to monitor changes in intraaxonal Na^+ concentration ($[Na^+]$) via changes in fluorescence. HSN imaging has obvious advantages for these studies. In contrast to VSD imaging, HSN imaging enables direct monitoring of local Na^+ influx. Moreover, the high spatial resolution of HSN imaging allows for detection of Na^+ influx in thin neuronal structures, such as axons, that are challenging to record with conventional microelectrodes. Assuming minimal differences in diffusion and geometry, this method provides a spatiotemporal readout of the integrated Na current that reveal differences in local Na^+ influx regardless of the underlying mechanism (i.e., differences in channel density or biophysical properties).

Most strikingly, Baranauskas et al. (8) are able to strongly dissociate the AP initiation site from the site of greatest Na^+ influx. According to the distribution of SBFI fluorescence intensities obtained with HSN imaging during single APs, the authors divided the entire AIS into three segments (S1–S3) (Fig. 1). They found that the $[Na^+]$ in S3 that includes the 10 μm of the trigger zone was about four-times lower than in the middle segment (S2) (Fig. 1). Note that differences in geometry, with a greater surface to volume ratio in S3 than in S2, would tend to increase final $[Na^+]$ in S3 if Na channel density and properties were uniform. This finding of greatest $[Na^+]$ in S2 indicated a clear spatial mismatch between the AP initiation site (S3) and the location with highest Na^+ influx. A qualitatively similar phenomenon of greater Na^+ influx in the middle of the AIS during trains of APs had been observed previously (13). However, the HSN imaging results obtained with single APs (18) provides higher spatiotemporal resolution that allows more precise localization of Na entry than during AP trains, in which the effects of diffusion would be greater. This lack of diffusion-dependent distortion of Na signals was also confirmed by the close temporal alignment of peak fluorescence signal and APs (figure S1 in ref. 8).

Finally, the authors evaluated the impact of differences in electrical load on the AP initiation site among the three AIS segments through computational modeling in the NEURON simulation environment. Because the S3 segment has the greatest distance from the soma, and the thinnest axonal diameter (19, 20) compared with S1 and S2, S3 has the greatest axoplasmic resistance isolating it from the somatodendritic compartments, which have a large membrane area and associated capacitive sink (Fig. 1). In addition, the thin, adjacent myelinated axonal membrane on the efferent side of S3 (distal to the soma) provides little capacitive sink. This combination of relative high internal resistance and low neighboring capacitive load imparts the S3 segment with the lowest capacitive load among the three axonal segments. In particular, the simulation results demonstrated in a biologically relevant model that, with the same Na current conductance, initiation occurs in the S3 segment, and that a decrease in S3 passive load through either an increase the physical distance to the soma or an increased axoplasmic resistance in the S1 segment lowers the AP threshold in S3. These computational results support the powerful role of electrical load in determining the initiation site of APs.

Most strikingly, Baranauskas et al. are able to strongly dissociate the AP initiation site from the site of greatest NA^+ influx.

Taking these data together, the present research represents a remarkable insight into spatial mismatch between the site of greatest Na^+ influx and the site of AP initiation, and provides experimental and computational evidence for a crucial role of cable properties in determining the AP initiation site. These results clearly indicate that the magnitude of Na^+ influx is not the only determinant in AP initiation and are consistent with a previous simulation study that suggested that axial resistivity and length were among the main determinants of the AP threshold (6). Importantly, the present research confirms that changes in factors associated with axonal cable properties would have profound impact on neuronal excitability and AP initiation.

1 Kole MH, Stuart GJ (2012) Signal processing in the axon initial segment. *Neuron* 73(2):235–247.
2 Bender KJ, Trussell LO (2012) The physiology of the axon initial segment. *Annu Rev Neurosci* 35:249–265.
3 Hodgkin AL, Rushton WA (1946) The electrical constants of a crustacean nerve fibre. *Proc R Soc Med* 134(873):444–479.
4 Johnston D, Wu SM (1996) *Foundations of Cellular Neurophysiology* (MIT Press, Cambridge MA).
5 Moore JW, Stockbridge N, Westerfield M (1983) On the site of impulse initiation in a neurone. *J Physiol* 336:301–311.
6 Mainen ZF, Joerges J, Huguenard JR, Sejnowski TJ (1995) A model of spike initiation in neocortical pyramidal neurons. *Neuron* 15(6):1427–1439.
7 Kress GJ, Dowling MJ, Eisenman LN, Mennerick S (2010) Axonal sodium channel distribution shapes the depolarized action potential threshold of dentate granule neurons. *Hippocampus* 20(4):558–571.
8 Baranauskas G, David Y, Fleidervish IA (2013) Spatial mismatch between the Na^+ flux and spike initiation in axon initial segment. *Proc Natl Acad Sci USA* 110:4051–4056.
9 Palmer LM, Stuart GJ (2006) Site of action potential initiation in layer 5 pyramidal neurons. *J Neurosci* 26(6):1854–1863.
10 Popovic MA, Foust AJ, McCormick DA, Zecevic D (2011) The spatio-temporal characteristics of action potential initiation in layer 5 pyramidal neurons: A voltage imaging study. *J Physiol* 589(Pt 17): 4167–4187.
11 Colbert CM, Johnston D (1996) Axonal action-potential initiation and Na+ channel densities in the soma and axon initial segment of subicular pyramidal neurons. *J Neurosci* 16(21):6676–6686.
12 Colbert CM, Pan E (2002) Ion channel properties underlying axonal action potential initiation in pyramidal neurons. *Nat Neurosci* 5(6):533–538.
13 Kole MH, et al. (2008) Action potential generation requires a high sodium channel density in the axon initial segment. *Nat Neurosci* 11(2):178–186.
14 Lai HC, Jan LY (2006) The distribution and targeting of neuronal voltage-gated ion channels. *Nat Rev Neurosci* 7(7):548–562.
15 Inda MC, DeFelipe J, Muñoz A (2006) Voltage-gated ion channels in the axon initial segment of human cortical pyramidal cells and their relationship with chandelier cells. *Proc Natl Acad Sci USA* 103(8):2920–2925.
16 Grubb MS, Burrone J (2010) Activity-dependent relocation of the axon initial segment fine-tunes neuronal excitability. *Nature* 465(7301):1070–1074.
17 Hu W, et al. (2009) Distinct contributions of Na(v)1.6 and Na(v) 1.2 in action potential initiation and backpropagation. *Nat Neurosci* 12(8):996–1002.
18 Fleidervish IA, Lasser-Ross N, Gutnick MJ, Ross WN (2010) Na+ imaging reveals little difference in action potential-evoked Na+ influx between axon and soma. *Nat Neurosci* 13(7):852–860.
19 Kole MH, Letzkus JJ, Stuart GJ (2007) Axon initial segment Kv1 channels control axonal action potential waveform and synaptic efficacy. *Neuron* 55(4):633–647.
20 Kim S, Guzman SJ, Hu H, Jonas P (2012) Active dendrites support efficient initiation of dendritic spikes in hippocampal CA3 pyramidal neurons. *Nat Neurosci* 15(4):600–606.